Two-dimensional clusters of identical bubbles

2001 J. Phys.: Condens. Matter 13 1395

(http://iopscience.iop.org/0953-8984/13/7/305)

INSTITUTE OF PHYSICS PUBLISHING JOURNAL OF PHYSICS: CONDENSED MATTER

J. Phys.: Condens. Matter **13** (2001) 1395–1411 www.iop.org/Journals/cm PII: S0953-8984(01)14761-2

Two-dimensional clusters of identical bubbles

M Fátima Vaz and M A Fortes

Departamento de Engenharia de Materiais, Instituto Superior Técnico, Lisboa, Portugal

Received 16 June 2000, in final form 6 November 2000

Abstract

We discuss in detail the assembly of two-dimensional identical bubbles in stable clusters. The clusters are classified into perfect and defective clusters, depending on the number of sides of their inner cells (defective clusters have inner cells with a number of neighbours different from 6). We evaluate the surface energy of clusters by a broken-bond method and compare with exact energy calculations for simple clusters. Special attention is given to perfect clusters which are classified by their symmetry. For particular values of the number of cells, N, called magic numbers, perfect clusters have special properties. We identify the clusters of smallest energy, for fixed number of cells N (minimal clusters). For large N the minimal clusters are perfect, but for small N a minimal cluster may be a defective cluster.

We produced two-dimensional clusters with N up to 15 by the 'monolayer foam' method and studied their relative incidence for $N = 6$.

1. Introduction

A foam is a cluster of soap bubbles, the energy of the cluster being smaller than the energy of the separated, spherical bubbles. The bubbles can assemble in various stable arrangements with different topologies and different free energies. The configurations of three-dimensional clusters have been determined only for clusters with 2 to 4 bubbles [1], for which the films are spherical. For larger numbers of cells, the clusters may have non-spherical films [2] and 'solving' them is not a simple problem. Two-dimensional (2D) clusters are simpler to analyse (circular films) and can be produced experimentally. Smith [3] discussed 2D free clusters of bubbles and gave examples of alternative topologies for fixed numbers of bubbles. He also prepared 2D confined clusters of bubbles for coarsening experiments.

This paper discusses in detail 2D clusters of N identical bubbles. We identify the stable clusters for given N and develop methods to estimate their surface energies. We pay particular attention to minimal clusters, defined as the clusters of smallest energy for fixed N. We also report experiments on 2D bubble clustering, in which N initially separated bubbles assemble in various arrangements.

The gas in and surrounding the cluster will be treated as incompressible. The area of a 2D bubble is thus invariant and independent of its association with other bubbles; and the total energy of a cluster reduces to its surface energy.

0953-8984/01/071395+17$30.00

The plan of the paper is as follows. Section 2 introduces various definitions and terms related to 2D clusters of identical cells (we use the term cell as synonymous with bubble) and classifies clusters into perfect and defective clusters. In perfect clusters all inner cells have six neighbours. Section 3, which discusses perfect clusters, introduces the broken-bond method for evaluating the energy of clusters. The energy is proportional to a broken-bond number, B, defined as the total number of missing neighbours of the peripheral cells of the cluster. Symmetry of perfect clusters and magic numbers are also discussed in section 3. Section 4 evaluates the energies of clusters of any type and fixed N and identifies the minimal clusters for each N. Section 5 describes the experimental technique used to prepare clusters and section 6 presents the experimental results. The final section contains the conclusions of this study.

The clusters under consideration in this paper are 'free' or isolated clusters, in the sense that the clusters do not contact solid surfaces. Clusters of the latter type can also be analysed and prepared by similar methods.

2. 2D clusters of identical bubbles; broken bonds

When N initially separated (circular) bubbles of the same area, A, assemble into a simply connected 2D cluster (figure 1(a)), the total length of films decreases; two adjacent bubbles

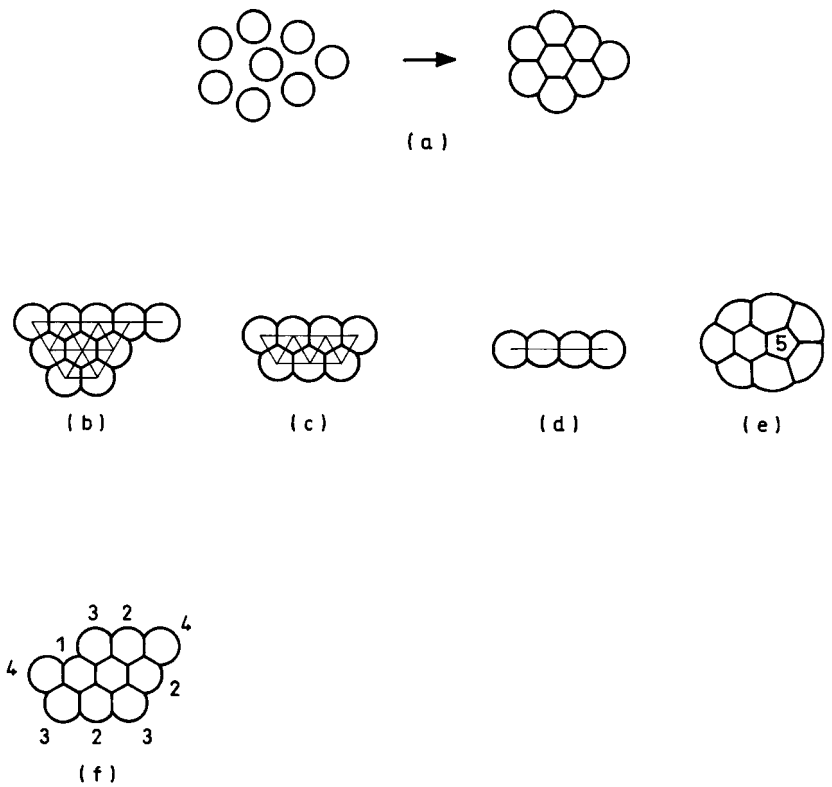

Figure 1. (a) Clustering of originally separated bubbles. (b)–(f) Various stable and unstable clusters. Cluster (e) is a defective cluster; the others are perfect clusters. Cluster (f) does not satisfy the rule of maximum row overlapping. We indicate the number of broken bonds of the peripheral cells of this cluster.

in the cluster share a common film. The N cells can assemble in various ways but we will consider only stable arrangements. The clusters prepared experimentally are all stable, in the sense that the cells remain in the same configuration when subjected to small perturbations (see section 5).

Triangulation is a necessary condition for cluster stability, according to our experimental observations. We construct the dual graph of the cluster by connecting the centre of each cell with the centres of adjacent cells, as in figures 1(b)–1(d). If no bonds dangle, triangulation is achieved and the cluster is stable (figures 1(a), 1(c), 1(e), 1(f)); otherwise the cluster is unstable (figures 1(b), 1(d)). A single row of connected cells is not stable (figure 1(d)) but two overlapping rows are stable (figure 1(c)).

(Stable) clusters fall into two classes: perfect clusters, in which all inner cells have $n = 6$ neighbours (these include clusters with no inner cells) and defective clusters, with at least one inner cell with $n \neq 6$. The stable clusters of figures 1(a), 1(c) and figure 2 are perfect; the one in figure 1(e) is a defective cluster with an inner five-sided cell.

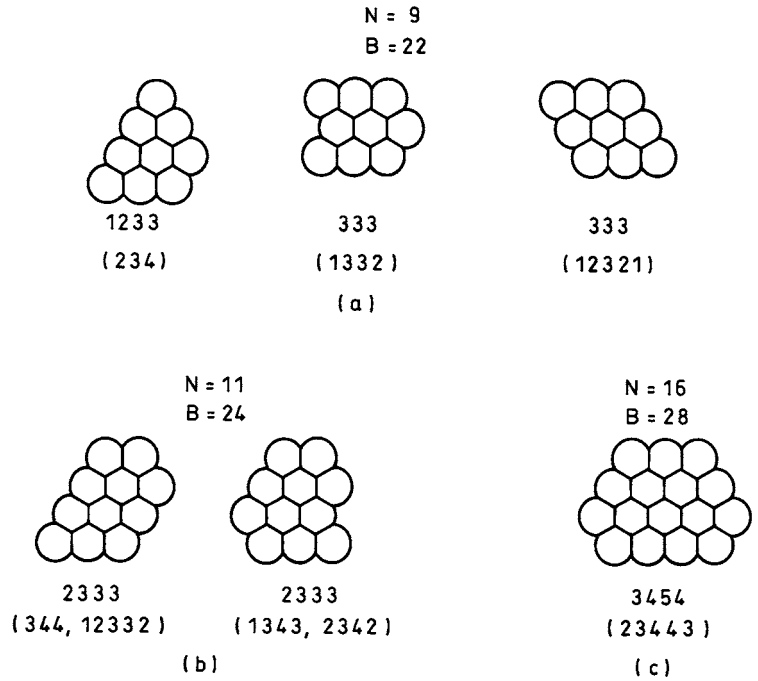

Figure 2. Perfect clusters with smallest bond number, B, for various values of N: $N = 9$, $B = 22$; $N = 11$, $B = 24$; $N = 16$, $B = 28$. We indicate the $\{N_i\}$ sequences. $N = 16$ is a magic number.

An infinite cluster of identical regular hexagonal cells forms a honeycomb. Each cell is surrounded by six cells and has six bonds with other cells. In a (finite) cluster, the peripheral cells (i.e., cells with a film not shared by another cell) in general have a number of neighbours $p < 6$. The total number of missing or broken bonds in the cluster is defined as

$$B = \sum (6 - p) \tag{1}$$

summed over all peripheral cells. We will use this number to evaluate the energy of a cluster or, more precisely, its excess energy in relation to that of the same number of cells of equal area, A, in a honeycomb. Figure 1(f) shows the numbers $(6 - p)$ of broken bonds for each peripheral cell in a cluster.

We can obtain the number of broken bonds of a cluster of N cells, of which I are internal and $P = N - I$ are peripheral, from the following equations:

$$B = 6 + 2N - (8 - \bar{n}_i)I = 6 + 2P + (\bar{n}_i - 6)I \tag{2}$$

where $\bar{n}_i$ is the average number of sides of the internal cells. We derive this by applying to the cluster of internal cells, which has trivalent vertices and d dangling edges, the following topological relation [4]:

$$\bar{n}_i = 6 - \frac{6 + E_p - 2d}{N} \tag{3}$$

where E_p is the number of peripheral edges of the inner cell cluster (obtained from the original cluster by removing the peripheral edges). Noting that $d = P$ and $B = 4p - E_p$, equation (2) follows.

For clusters with $\bar{n}_i = 6$ and, in particular, for perfect clusters, equation (2) simplifies to

$$B = 6 + 2P. \tag{4}$$

For large perfect clusters, the average number of broken bonds per peripheral cell, B/P, is 2.

The cluster of smallest energy for given N will be termed the minimal cluster. Broadly, we expect minimal clusters to have smaller values of B, but they may not because defects in the cluster alter the average bond energy in the cluster. This will be discussed in detail in section 4. For perfect clusters, B provides a simple evaluation of the cluster energy and can be used in the search for minimal clusters of this type. Therefore, we will first analyse perfect clusters.

3. Perfect clusters

3.1. Description of perfect clusters

We describe a perfect cluster (P cluster) as formed by R successive close-packed rows of cells, each with N_i cells. The cluster has a packing sequence $\{N_i\}$. In drawings of clusters, we place the rows horizontally with row 1 at the top and row R at the bottom. A P cluster in general has three different $\{N_i\}$ descriptions, because it has close-packed rows in three orientations (examples are given in figure 2(b)). In addition, a given $\{N_i\}$ sequence does not in general define a unique cluster because the successive rows can pack in different ways (figure 2). The $\{N_i\}$ sequence is nevertheless convenient to use in discussing low-energy P clusters.

3.2. Broken-bond number of perfect clusters

Packing the successive rows with maximum overlap reduces the energy of clusters with a given $\{N_i\}$ sequence, since overlap reduces the B-number of the cluster. The cluster of figure 1(f) does not satisfy the condition of maximum row overlap. In the following, we consider only this type of cluster and $\{N_i\}$ sequences with maximum overlap.

The maximum B for a fixed N in (stable) perfect clusters occurs for the cluster formed by two overlapping rows of cells with a $\{2, 2, \ldots, 2\}$ sequence as in figure 1(c). The bond number is

$$B_{max} = 4N + 2. \tag{5}$$

Determination of the minimum B for given N is not simple. The $\{N_i\}$ sequence of a P cluster of minimum B has $\Delta N_i = 0, \pm 1$ which minimizes the number of peripheral cells (cf. (4)). For these clusters, the number of peripheral cells is $2R - 4 + N_1 + N_R$ and

$$B = 2(2R + N_1 + N_R) - 2. \tag{6}$$

It is convenient to define *regular* $\{N_i\}$ sequences formed by two half-sequences of successive integers for which all $\Delta N_i = \pm 1$ (for example, $\{2, 3, 4, 5, 6, 5, 4\}$). Equation (6) of course applies to such clusters. The general form of a regular $\{N_i\}$ sequence is

$$\{i, i+1, \ldots, i+n, \ldots, i+n-m\} \qquad n \geqslant m. \tag{7}$$

The largest N_i is $i+n$. The sequence defines a unique cluster. To obtain the number N of cells in the cluster we note that

$$\sum_{k=1}^{n} k = \frac{n^2+n}{2} \tag{8}$$

where k is an integer. The result is

$$2N = (2i+n)(n+1) + (2i+2n-m-1)m. \tag{9}$$

The number R of rows in the sequence (7) is

$$R = n + m + 1 \tag{10}$$

and the broken-bond number, B, is

$$B = 2(2i+3n+m+1). \tag{11}$$

Before proceeding with the identification of the P clusters of smallest energy, we classify P clusters according to their symmetry.

3.3. Symmetry of P clusters

Perfect clusters can be classified according to their (maximum) symmetry into four classes: (A) clusters with a sixfold axis of symmetry; (B) clusters with a threefold axis of symmetry; (C) clusters with a plane of symmetry; (D) clusters with no symmetry. Class (C) includes clusters with two symmetry planes (and therefore a twofold axis of symmetry) and class (D) includes clusters with a centre of symmetry. Figure 3 shows examples of each type. Defective clusters can also be classified by symmetry, but this will not be considered.

Turning to P clusters with regular $\{N_i\}$ sequences, the symmetry classes defined above associate with the following sequences, which are particular cases of the general form (7):

(1) For

$$N = m = i - 1$$

the $\{N_i\}$ sequence is

$$\{i, i+1, \ldots, 2i-1, \ldots, i+1, i\}$$

with

$$\begin{aligned} N &= 3i^2 - 3i + 1 \\ R &= 2i - 1 \\ B &= 12i - 6. \end{aligned} \tag{12}$$

These clusters have a sixfold axis of symmetry and thus only one $\{N_i\}$ description.

(2) For

$$m = i - 1 \qquad n \neq i - 1$$

the $\{N_i\}$ sequence is

$$\{i, i+1, \ldots, i+n, \ldots, n+1\}$$

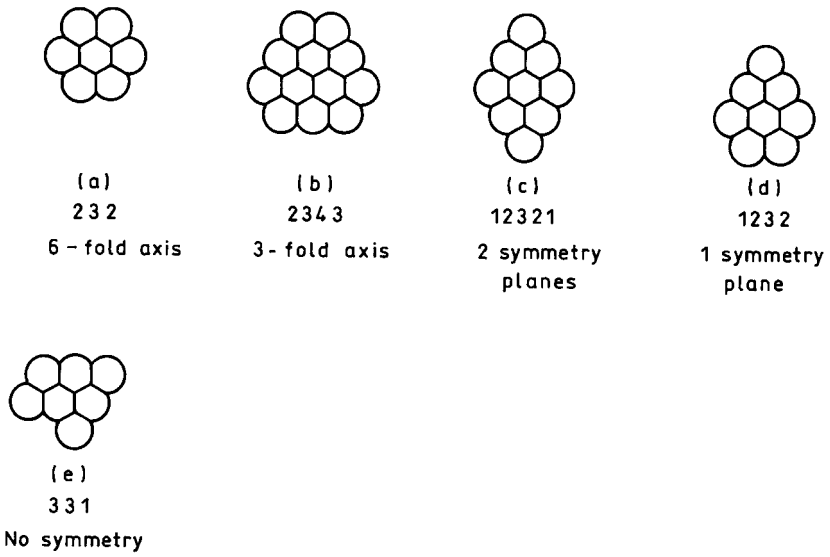

Figure 3. Examples of perfect clusters of the various symmetry classes defined in the text. We indicate the $\{N_i\}$ sequences.

with

$$\begin{aligned} 2N &= (2i+n)(n+1) + (i+2n)(i-1) \\ R &= i+n \\ B &= 6i+6n. \end{aligned} \tag{13}$$

These clusters have a threefold axis of symmetry and only one $\{N_i\}$ sequence.

(3) For

$$m \neq n \qquad m \neq i-1$$

the $\{N_i\}$ sequence is the one given in (7) with N, R and B given by (9)–(11). These clusters have a plane of symmetry and two equivalent $\{N_i\}$ sequences. The second $\{N_i\}$ sequence is, in general, not regular.

3.4. Magic numbers

Particular values of N have regular $\{N_i\}$ sequences that define clusters with special properties, which we will term magic numbers and magic clusters, respectively. The special properties are:

(1) A magic N has only one P cluster with minimum number, B, of broken bonds.
(2) For a magic N (but not for any other N), increasing the number of cells by one increases the broken-bond number, B, by two.
(3) The $\{N_i\}$ sequence of a magic cluster is regular with N_1 and N_R equal or differing by unity.

We searched for magic numbers and their properties empirically.

Introducing property 3 in the general form (7) of a regular sequence determines the magic numbers listed in table 1 as a function of a single parameter k (integer $\geqslant 1$). The table contains the regular $\{N_i\}$ sequence, R, B and the symmetry of the magic clusters. The B is the smallest

Table 1. Magic numbers and magic clusters.

N	$\{N_i\}$ regular sequence	R	B	Symmetry	N $(k=2)$	$\{N_i\}$ regular sequence $(k=2)$
$3k^2-3k+1$	$k,\ldots,2k-1,\ldots,k$	$2k-1$	$12k-6$	6	7	232
$3k^2-2k^{(*)}$	$k-1,\ldots,2k-1,\ldots,k$	$2k-1$	$12k-4$	P	8	1232 (233)
$3k^2-k$	$k+1,\ldots,2k,\ldots,k+1$	$2k-1$	$12k-2$	P	10	343 (2332)
$3k^2$	$k,\ldots,2k,\ldots,k+1$	$2k$	$12k$	3	12	2343
$3k^2+k$	$k,\ldots,2k,\ldots,k$	$2k$	$12k+2$	P	14	23432 (3443)
$3k^2+2k$	$k+1,\ldots,2k+1,\ldots,k+2$	$2k$	$12k+4$	P	16	3454 (23443)
$3k^2+3k+1$	$k+1,\ldots,2k+1,\ldots,k+1$	$2k+1$	$12k+6$	6	19	34543

* Except for $k=1$.

possible for a P cluster with N cells (property 1). The table also gives an example of the $\{N_i\}$ sequences for $k=2$ (in brackets we give the equivalent sequence, if one exists).

For an N that is not in table 1, the smallest B is equal to that of the following magic number (property 2). These non-magic numbers have, in general, more than one P cluster of lower energy which may have threefold symmetry (but not sixfold symmetry), a plane of symmetry or no symmetry. Figure 2 shows examples of the P clusters of smallest B for $N=9$, $N=11$ and $N=16$. Of these, only the cluster for $N=16$ is magic.

Figure 4 shows the smallest number of broken bonds per cell in the cluster, B/N, plotted as a function of N. It tends to decrease as N increases. But for $N>14$, B/N always increases following a magic number (arrows in figure 4).

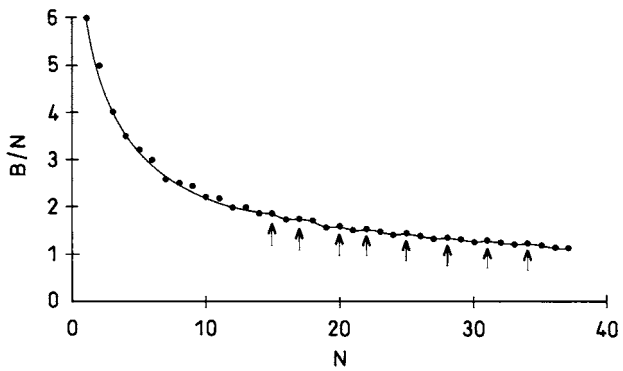

Figure 4. The variation of the broken-bond number per cell, B/N, as a function of N for perfect clusters. The ratio B/N increases following a magic number for $N>14$ (arrows).

The minimum bond number B for large N (large k in table 1) is of the order of $12k$ while $N \cong 3k^2$. Thus

$$B_{min} = 4\sqrt{3}N^{1/2} \tag{14}$$

which can be compared with the maximum bond number, namely $B_{max}=4N$, for large N (equation (5)).

4. The energy of clusters

We obtain the surface free energy, E_c, of a 2D cluster (per unit length normal to the plane of the cluster) by multiplying the total length of films by the film tension, γ. We neglect the

contributions to the free energy of the triple junctions (Plateau borders) and of the gas in the bubbles (incompressible gas). An exact calculation of the total film length requires 'solving' the cluster, by determining the radii and subtended angles of all films, for given topology and areas of the cells (circular films meeting at 120° at triple junctions and equilibrium of pressures). Such calculations can be rather complicated since they require solving complex trigonometric equations. We solved only simple clusters (see appendices 1 and 2).

To avoid the exact solution, we estimate the energy of a cluster on the basis of the number of broken bonds. Instead of E_c, we use the excess energy, E, of the cluster:

$$E = E_c - E_0 \qquad E_0 = 3Na\gamma \tag{15}$$

where E_0 is the energy of the same number of cells (of the same area) in a honeycomb. a is the edge length of a honeycomb cell of area A:

$$A = \frac{3\sqrt{3}}{2}a^2. \tag{16}$$

4.1. Energy of perfect clusters

We obtain the excess energy E of a perfect cluster from

$$E = B\varepsilon(6) \tag{17}$$

where $\varepsilon(6)$ is the average energy per broken bond. The (6) indicates a perfect cluster.

Appendices 1 and 2 show that for perfect clusters $\varepsilon(6)$ is weakly dependent on the topology and size (number of cells, N) of the cluster, although it tends to increase slightly with size. Table 2 lists the calculated values of $\varepsilon(6)$ for a number of perfect clusters identified in figure 5.

Table 2. Calculated broken-bond energies for the simple perfect clusters of figure 5.

Number of cells in cluster, N	Total number of broken bonds, B	$\varepsilon(6)$ ($a\gamma$ units)
1	6	0.452
2	10	0.425
3	12	0.431
4	14	0.432
7	18	0.439
13	30	0.447

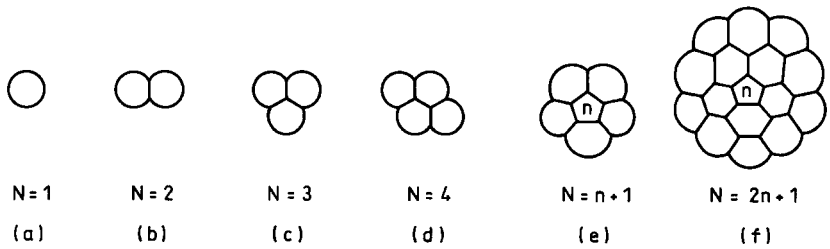

Figure 5. Clusters for which we made exact energy calculations. For the last two clusters we made calculations for $3 \leqslant n \leqslant 9$.

In our search for minimal clusters and in the calculations of the energies of the perfect clusters obtained experimentally, we used the bond energy

$$\varepsilon(6) = 0.447a\gamma \qquad \text{(perfect clusters)} \tag{18}$$

for the $N = 13$ cluster of table 1. Within this approximation, perfect clusters with the same broken-bond number B, such as the clusters of figure 2 for $N = 9$ and $N = 11$, have the same energy.

4.2. Energy of defective clusters

We will discuss two methods for evaluating the excess energy E of a defective cluster. Both calculate the energy from the number of broken bonds, B. The first method is more appropriate for large clusters while the second applies to smaller clusters, with, say, $N < 22$. A defective cluster will be characterized by a number S, termed the power of the cluster:

$$S = \sum_{\text{inner cells}} (n_i - 6) = I(\bar{n}_i - 6) \tag{19}$$

where the n_i are the numbers of sides of inner cells and I is the total number of inner cells. We write the number of broken bonds, B, given by (2), as

$$B = 6 + 2P + S. \tag{20}$$

For fixed defective content (e.g. one 5-cell; two 7-cells; etc), we identify the clusters of smallest B for each N. The B versus N sequences for these defective clusters of smallest energy of course differ from the one for perfect clusters, but again show jumps (by 2) following particular values of N. For example, for clusters with a single 5-cell the jumps follow $N = 6, 7, 9, 11, 13, 16, 18, 21, \ldots$ (the values for perfect clusters are the magic numbers: 5, 7, 8, 10, 12, 14, 16, 19, 21, ...). No simple rules give these numbers for defective clusters of smallest energy. Instead we found them for $N < 22$ by drawing all defective clusters with given defect content.

For clusters with smallest energy, the difference between the smallest B-values of perfect and defective clusters with fixed defect content fluctuates around an average constant value as N changes. For fixed N, the smallest B for perfect clusters is larger than the smallest B for a defective cluster of fixed S for $S > 0$ and smaller for $S < 0$.

The first method for estimating the excess energy, E, of defective clusters, calculates the energy from

$$E = B\varepsilon(6) + \Delta E_d \tag{21}$$

where B is the broken-bond number of the cluster and we take the average energy of a broken bond equal to the value $\varepsilon(6)$ given in (19). The extra energy ΔE_d is a (positive) strain energy due to the defects.

To estimate ΔE_d, we applied our previous analysis [5] of the strain energy of defects embedded in a honeycomb which is suitable for large equiaxed (round) clusters of small bond number B, with central defects.

For $S = 0$ the defect is a pure dislocation and has an associated Burgers vector b (a lattice vector of the hexagonal honeycomb lattice). For example, a pair of adjacent 5- and 7-cells has a unit Burgers vector, i.e. a vector between the centres of adjacent hexagonal cells, with $b^2 = 3a^2$; an adjacent 4–8 pair and a 5–7 pair connected by an extra edge have $b^2 = 9a^2$; etc.

The strain energy density, w, due to a dislocation b in a honeycomb is [5]

$$w = \frac{G}{4\pi^2}\frac{b^2}{r^2} \tag{22}$$

where G is the shear modulus of the honeycomb:

$$G = \frac{1}{2\sqrt{3}}\frac{\gamma}{a}$$

and r is the distance to the defect. For a fairly round cluster of outside radius r_1, the extra energy ΔE_d due to the dislocation defect will be

$$\Delta E_d = \int_{r_0}^{r_1} 2\pi r w(r)\, \mathrm{d}r = \left(\frac{\sqrt{3}}{4\pi}\lambda \ln \frac{r_1}{r_0}\right) a\gamma \tag{23}$$

where $\lambda = b^2/(3a^2)$ and r_0 is the core radius of the dislocation. Taking $r_1/r_0 \cong (N/2)^{1/2}$ yields

$$\Delta E_d = \frac{\sqrt{3}}{4\pi}\lambda \ln\left(\frac{N}{2}\right)^{1/2}. \tag{24}$$

This equation can be used to estimate the contribution of dislocations to the cluster energy. We expect its accuracy to increase as N increases in fairly round clusters, but have not tested this.

Given a defective cluster with $S = 0$, there is a perfect cluster with the same N and B and $\Delta E_d = 0$ which has lower energy. In the search for minimal clusters, we discard defective clusters with $S = 0$. We also discard clusters with $S > 0$, since, for the same N, there is a perfect cluster of smaller B with $\Delta E_d = 0$.

The situation differs for defective clusters with $S < 0$ because they can have smaller B than a perfect cluster with the same N. However, the clusters with $S < 0$ that have to be considered should have pure disclination character (for example, a single 5-cell or a 5–5 pair). Clusters with $S < 0$ with mixed dislocation/disclination character (for example, 5–5–7 cells) cannot be minimal clusters since replacement of the dislocation (the 5–7 pair, in the example) by 6-cells reduces the energy at constant N.

For a pure disclination in a honeycomb, the strain energy density is [5]

$$w = \frac{GS^2}{36} \tag{25}$$

independently of r. The extra strain energy due to a disclination of strength S in a cluster of N cells is then

$$\Delta E_d = \frac{NS^2}{48} a\gamma. \tag{26}$$

We used this equation to calculate the energies of disclinated clusters and compared them with exact calculations for one-shell and two-shell clusters with a central n-cell (appendix 2). For $n < 6$ ($S < 0$), equations (21) and (26) underestimate the excess energy, E, of the cluster by factors of 1.1 for $n = 5$ and 1.4 for $n = 3$; for $n > 6$ ($S > 0$), the reverse happens (a factor of 1.1 for $n = 7$ and of 1.4 for $n = 9$). Because (21) and (26) overestimate the energy for $n > 6$, we cannot rule out clusters with $S > 0$ disclination defects as minimal clusters.

Our second method for evaluating the energy of defective clusters applies to relatively small clusters with a single cell with $n \neq 6$. Instead of using the bond energy $\varepsilon(6)$, we use a bond energy $\varepsilon(n)$ for each value of n and calculate the energy of a cluster with an n-cell from

$$E = B\varepsilon(n). \tag{27}$$

The $\varepsilon(n)$ come from the exact calculations of appendix 2 for round clusters with a central n-cell and two surrounding shells of cells (see table A1 in appendix 2). Table 3 gives the $\varepsilon(n)$. They are slightly larger than the corresponding values that can be obtained for one-shell clusters.

The energy of defective clusters of pure disclination character with pairs of cells $n \neq 6$ can be estimated from (27) using the $\varepsilon(n)$ for $n = 6 - S$. For example, for a cluster with a 5–5 pair we use $\varepsilon(4)$ in (27).

Table 3. Broken-bond energies $\varepsilon(n)$ in clusters with an n-cell.

n	$\varepsilon(n)$
3	0.794
4	0.592
5	0.495
6	0.447
7	0.414
8	0.404
9	0.399

4.3. Identification of minimal clusters

Different clusters of given N may have similar values of the energy. Among the clusters calculated in appendices 1 and 2 there are two pairs of clusters with the same N. For $N = 4$, the cluster with a 3-cell surrounded by 3-cells has a total energy $E_c = 19.07\, a\gamma$, while the cluster with two rows of two cells has $E_c = 18.26\, a\gamma$. For $N = 10$, the cluster with a central 9-cell surrounded by 9-cells has energy $E_c = 40.44\, a\gamma$, while a 3-cell surrounded by 2-shells has $E_c = 41.92\, a\gamma$.

These small differences in energy make the identification of minimal clusters, using approximate methods, uncertain. However, a few guidelines help in this search. A minimal cluster is either a perfect cluster or a cluster with pure disclination character, and any defective cell in the cluster must have either $n < 6$ or $n > 6$.

We have used (27) with the values of $\varepsilon(n)$ of table 3 to identity the minimal clusters for $N < 22$. The clusters in competition were perfect clusters, clusters with a single n-cell with $3 \leqslant n \leqslant 9$ and clusters with a pair of 5-cells or a pair of 7-cells. Other pairs (e.g. 4–8 and 3–9) have energies that are too high.

Table 4 gives the minimal clusters identified in this way with their excess energies, E, obtained from (27). We also indicate clusters with the same N and excess energies E differing by less than 1% from the minimum. (The smallest E is listed first, in bold type.) For $N = 20$ and $N = 22$, which are not magic numbers, there are two or more P clusters with the smallest B, among clusters with the same N. These clusters have the same minimal energy within the approximate methods used.

Equations (21) and (26) suggest that, for larger N, the minimal clusters are likely to be perfect clusters. However, equation (27) favours defective clusters with $n > 6$ cells for large N.

Table 4. Minimal clusters and excess energies for $N \leqslant 22$. (Note: (n) indicates a cluster with one n-cell. P indicates a perfect cluster.)

N	Minimal cluster	Excess energy, E ($a\gamma$ units)	N	Minimal cluster	Excess energy, E ($a\gamma$ units)
1	**P**	**2.68**	12	**P**	**10.73**
2	**P**	**4.47**	13	**(7)**	**11.18**
3	**P**	**5.36**	14	**P**	**11.62**
4	**P**	**6.26**	15	**(7)**	**12.01**
5	**(4)** P	**7.10**; 7.15	16	**(5)**	**12.38**
6	**(5)**	**7.43**	17	**(7)**	**12.83**
7	**P**	**8.05**	18	**(5)** P	**13.37**; 13.41
8	**(7)**	**8.69**	19	**P**	**13.41**
9	**(5)**	**9.41**	20	**P** (5)	**14.30**; 14.36
10	**P**	**9.83**	21	**P** (5)	**14.30**; 14.36
11	**(7)**	**10.35**	22	**P** (7) (5)	**15.20**; 15.32; 15.34

5. Experimental method

The method used to prepare 2D clusters is a variant of the one used to obtain 'monolayer' foams [6, 7]. We formed identical bubbles (volume around 10 mm^3) by blowing air into a solution, through a capillary. As the bubbles come to the surface, they are sandwiched between the solution surface and a parallel plate above it, at a separation of a few millimetres. The areas of the bubbles at the plate are around 5 mm^2. When formed near each other, they rapidly assemble into an essentially 2D cluster due to long-range attractive capillary forces between the bubbles, caused by the liquid menisci at their bottoms, just as in Bragg bubble rafts [8].

Tilting the vessel which contains the solution makes the separation between the solution surface and the plate non-uniform: the cluster moves to the region where that separation is smallest and the liquid fraction in the cluster (i.e. in the Plateau borders and films of the cluster) increases. In the experiments, we increased the tilting angle until the cluster lost rigidity [9] and separated into individual randomly arranged bubbles (figure 6(a)) embedded in a large 'pond' of liquid solution in contact with the plate. Levelling the vessel, the liquid 'pond' disappears and the separated bubbles reassemble into varying clusters, as in figures 6(b)–6(e) for $N = 6$. The clusters are very stable against shaking the vessel or gently pushing a bubble with a (submerged) rod.

6. Experimentally observed clusters

The photographs of figures 6–8 show examples of cluster configurations for various N. Figure 6 shows all configurations observed for $N = 6$. Figure 7 illustrates various single-defective clusters for $N = 15$. The clusters of figure 8 contain a pair of adjacent 5/7-cells (figure 8(a)) or a 5–7 pair connected by an extra edge (figure 8(b)). Most defective clusters obtained experimentally had inner cells with five and seven sides; a few clusters had cells with $n = 4$ and $n = 8$; we never observed cells with three or $\geqslant 9$ sides. We found the minimal clusters of table 4 for all N-values experimentally investigated. These experimental results show that several cluster configurations occur for fixed N, including configurations of relatively high energy.

Because of the relatively small height of the bubbles, the Plateau borders at the plate are large and give, in some photographs, the wrong impression of a double film between adjacent cells. In fact, a single film separates adjacent cells in the final configuration. We could obtain drier clusters by increasing the gap between plate and solution using bubbles of larger volume, which are, however, difficult to form with uniform size.

Inner cells frequently seem to be smaller (smaller area at the top plate) because the height of the menisci at the solution tends to be smaller in the inner cells than in the peripheral cells, of lower pressure. The 4-cell in the cluster of figure 8(b) provides an example.

Our cluster preparation method favours relatively round clusters. For example, although two-row stable clusters (as in figure 1(c)) easily form as a Bragg raft, they are not stable in the monolayer clusters; when we put the plate on top of a two-row Bragg cluster, it transforms into a round cluster.

We recorded the incidence of the different clusters for $N = 6$ in an attempt to correlate their frequency with energy. Figure 9 shows the frequency of clusters obtained for $N = 6$ (clusters 1 to 4) plotted as a function of their estimated energies, for 25 clusters. The frequency and energy weakly correlate. The frequency and the initial positions of the separated bubbles might also correlate. To check such a correlation we shook six coins inside a circular frame and determined the Voronoi partition of the circle based on the final positions of the coins. Figure 9 shows the results for 25 trials. The correlation with experiment is again weak; two

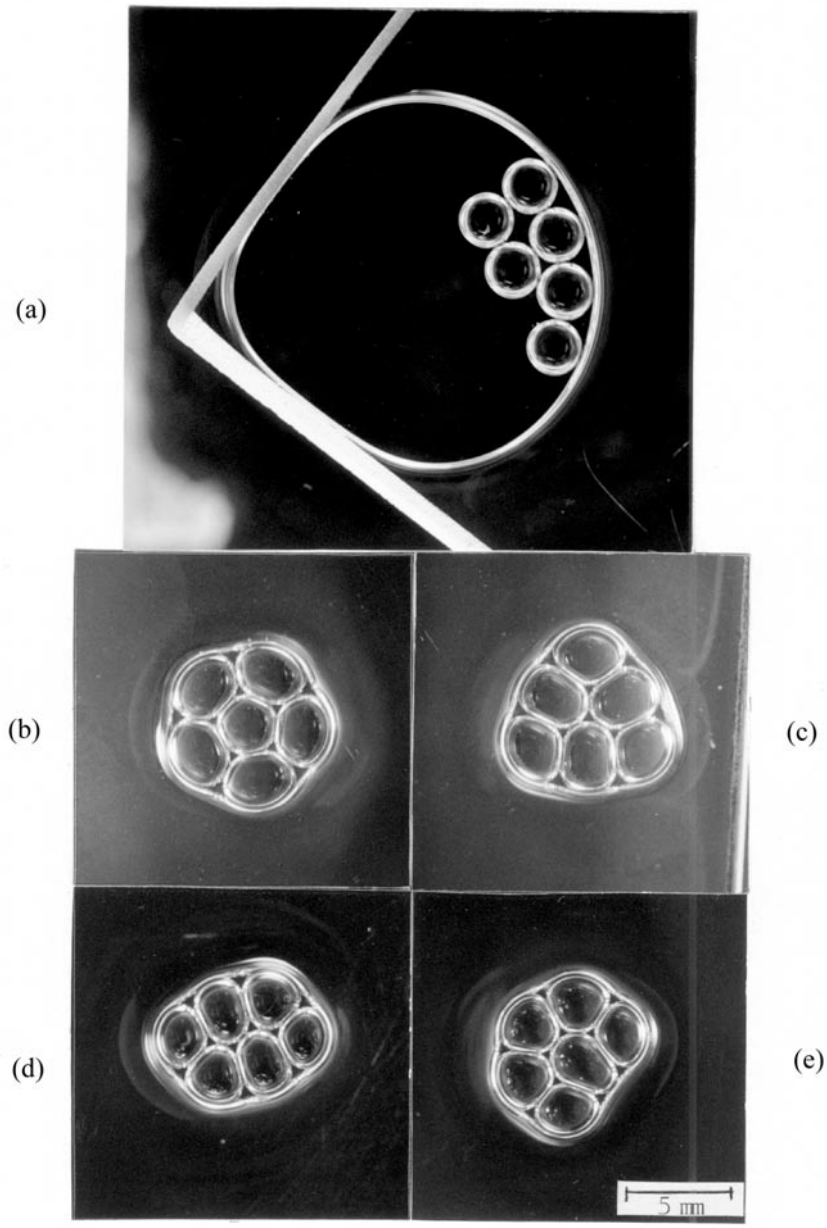

Figure 6. (a) Six originally separated bubbles in a monolayer. The bubbles are 'immersed' in a large liquid region bounded by an outer interface with air; (b)–(e) the four clusters experimentally observed for $N = 6$ bubbles.

of the coin clusters (5 and 6) were not observed with bubbles and the frequency of cluster 4 is much larger than in the actual clusters. Probably the capillary forces in the experiment favour the 'transformation' of the higher-energy Voronoi clusters 5 and 6, and also 3 and 4 of figure 9, into a cluster 2. The dynamic problem of bubble assembly is, however, beyond the scope of this study.

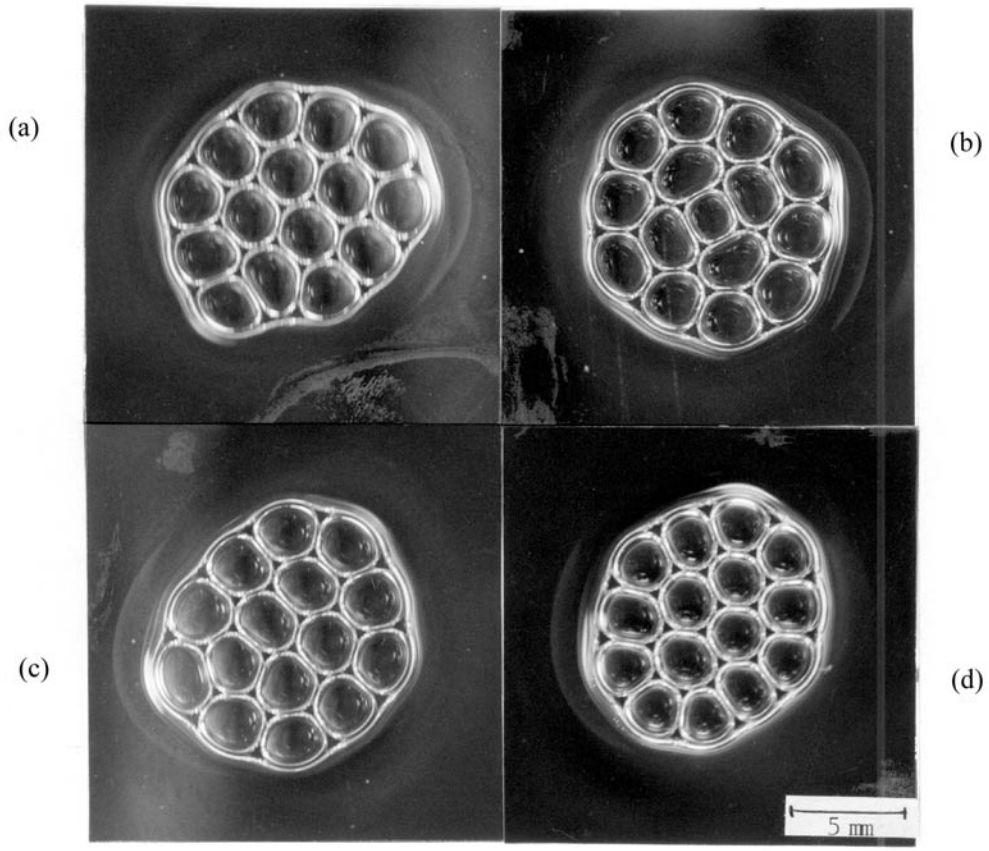

Figure 7. Clusters with $N = 15$ cells: (a) perfect cluster; clusters with: (b) a 4-cell; (c) a 5-cell; (d) a 7-cell. The minimal cluster is (d).

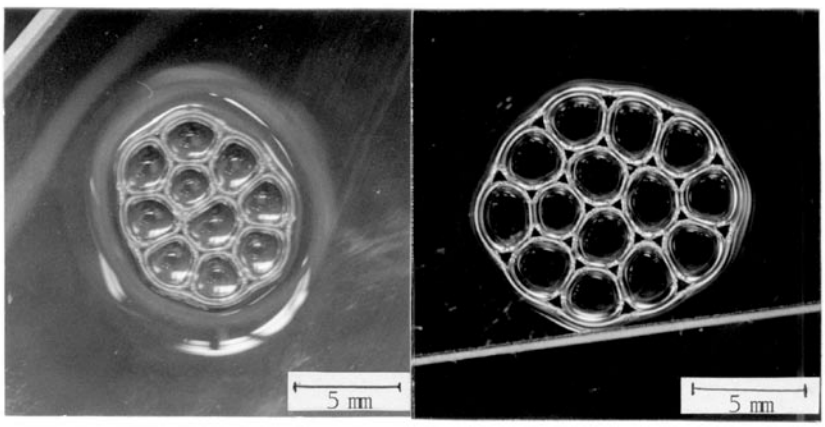

Figure 8. Clusters with a pair of 5- and 7-cells: (a) adjacent; (b) separated.

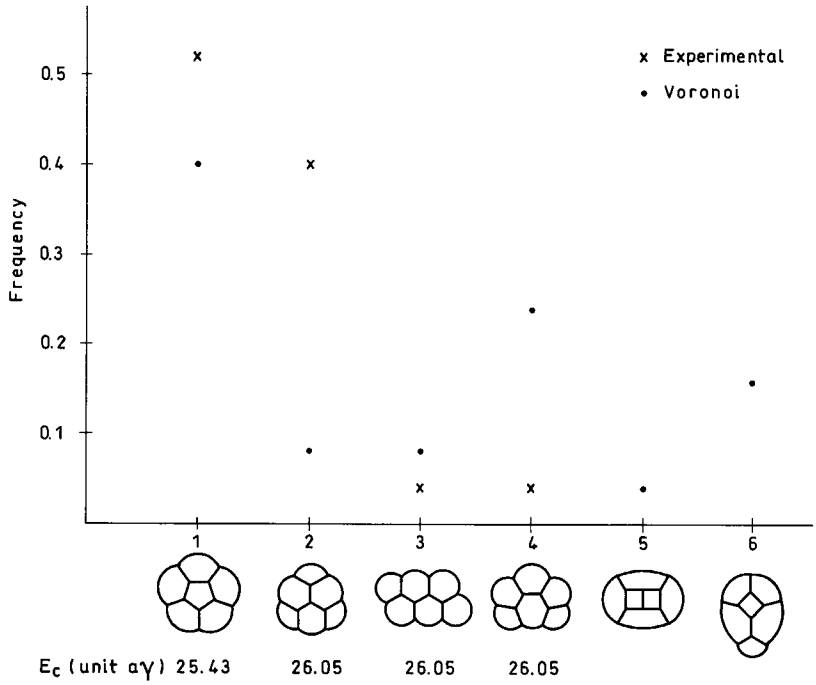

Figure 9. The frequency of occurrence of clusters with $N = 6$: $\times$: experimental; ●: simulation based on a Voronoi partition of a circle. We obtained only clusters 1 to 4 in experiments. The estimated total energies of these clusters are indicated.

7. Conclusions

Isolated bubbles may assemble in various stable (metastable) clusters of lower energy. These clusters differ in their topology and energy. We classified the clusters as perfect and defective clusters (when inner cells have a number of sides $n \neq 6$) and discussed their general properties. We analysed perfect clusters in detail, and described them by a sequence of numbers $\{N_i\}$. For particular numbers of bubbles, N, called magic numbers, the perfect clusters have special properties.

We calculated the (surface) energy of clusters by a broken-bond approach. The contribution of the gas to the energy was neglected since we assumed the incompressibility of the gas in the bubbles. If the gas is compressible, its contribution to the free energy depends on pressure, p, and increases as p increases (at constant temperature, T). Assuming ideal-gas behaviour, the free energy is $RT \ln p$ per mole, where R is the gas constant. The total free energy of the (ideal) gas in a 2D cluster is then $\sum p_i A_i \ln p_i$, where A_i and p_i are the area and gas pressure in bubble i. To calculate this would require solving the clusters to obtain A_i and p_i for a fixed amount of gas in each bubble (i.e., fixed numbers of moles).

For perfect clusters, the (surface) energy is simply proportional to the number of broken bonds. For defective clusters, we must add a strain energy term. Alternatively, we can use a specific bond energy for each type of defective cluster to calculate the energy of relatively small clusters of low energy. We assessed the accuracy of the broken-bond method by comparing its results to exact calculations of the cluster energies for simple clusters.

We tentatively identified the clusters of smallest energy for each N (minimal clusters) using the second method to obtain the energies of defective clusters. For $N \leqslant 22$, the minimal

clusters are those indicated in table 4. For larger N, the minimal clusters are either perfect or contain cells with $n > 6$, but our calculations of energies are not accurate enough when it comes to the identification of minimal clusters.

We produced clusters experimentally with a special technique, by assembling N initially separated bubbles. In general, these clusters tend to be 'round', of relatively low energies, including the minimal cluster. Nevertheless, the incidence of the various clusters for fixed N weakly correlates only with energy and is probably determined by the attractive forces between the originally separated bubbles and by their initial positions.

The findings of this study may be relevant to biological epithelial tissues formed by identical cells and to biological processes such as cell sorting [10].

The paper concentrated on the self-assembly of 2D identical bubbles. For 2D bubbles of different sizes, the number of possible clusters for a given set of cells increases considerably and the analysis becomes much more complicated. Extension to 3D is also possible, but again the complexity will greatly increase.

Acknowledgment

The authors wish to thank Professor J Glazier for his critical reading of the manuscript.

Appendix 1. Energy of simple perfect clusters

To estimate the bond energy of perfect clusters and assess the accuracy of the broken-bond method, we calculated exactly the total lengths of films for a few simple clusters. We give an example of the actual calculations for the cluster of three cells (shown in figure 5(c)) which has threefold symmetry.

The equilibrium condition of 120° angles at triple points implies

$$R = b \tag{A.1}$$

where R is the radius of curvature of the outer films and b is the length of an inner film. The inner films are straight, by symmetry. The area of one cell is

$$A = \left(\frac{\pi}{2} + \frac{1}{\sqrt{3}}\right)R^2. \tag{A.2}$$

The edge length, a, of a cell of the same area, A, in a honeycomb ($A = 3\sqrt{3}/2a^2$) is

$$a = \frac{1}{3}(\sqrt{3}\pi + 2)^{1/2}R. \tag{A.3}$$

The total length of the films is

$$L = 3(b + \pi R) = 6R\left(\frac{1}{\sqrt{3}} + \frac{\pi}{2}\right) \tag{A.4}$$

or, introducing a,

$$L = 6\left[\frac{3\sqrt{3}}{2}\left(\frac{1}{\sqrt{3}} + \frac{\pi}{2}\right)\right]^{1/2} = 14.1795\, a. \tag{A.5}$$

The energy of the cluster is $L\gamma$ and the bond energy is, for three cells and twelve broken bonds,

$$\varepsilon_b = \frac{L - 3x3a}{12}\gamma = 0.4312\, a\gamma. \tag{A.6}$$

We can also easily calculate for clusters of one and two cells (figures 5(a), 5(b)). For the cluster of four cells in figure 5(d), the calculation is more complicated. This cluster has

three curved films meeting at triple points; the equilibrium of pressures relates their radii of curvature. Determination of the cluster requires numerical solution of one trigonometric equation.

Appendix 2. Energy of defective clusters

We solved clusters formed by a central n-cell surrounded by one or two shells of 6-cells (figures 5(e), 5(f)). The solution for one shell is relatively simple. For two shells we must solve a system of four trigonometric equations with four unknown quantities. Table A1 indicates our main result (i.e. the total perimeter of the films in the cluster). The details of the calculations will not be given.

Table A1. Total film length of one-shell and two-shell clusters with one central n-cell.

	Total film length*	
n	One shell	Two shells
3	19.073	41.916
4	22.158	50.844
5	25.430	60.371
6	28.897	70.415
7	32.561	80.494
8	36.410	91.151
9	40.443	102.333

* In units of the edge length a of a honeycomb cell of the same area A as the cells in the cluster ($A = (3\sqrt{3}/2)a^2$).

References

[1] Herdtle T and Aref H 1991 *Proc. R. Soc.* A **434** 441
[2] Weaire D and Hutzler S 1999 *The Physics of Foams* (Oxford: Clarendon) Appendix C
[3] Smith C S 1952 *Metal Interfaces* (Cleveland, OH: ASM) p 65
[4] Fortes M A and Ferro A C 1985 *Acta Metall.* **33** 1697
[5] Fortes M A and Vaz M F 1998 *J. Phys.: Condens. Matter* **10** 7519
[6] Vaz M F and Fortes M A 1997 *J. Phys.: Condens. Matter* **9** 8921
[7] Rosa M E and Fortes M A 1998 *Europhys. Lett.* **41** 577
[8] Shi L T and Argon A S 1982 *Phil. Mag.* A **46** 255
[9] Bolton F and Weaire D 1990 *Phys. Rev. Lett.* **65** 3449
[10] Glazier J and Graner F 1993 *Phys. Rev.* E **47** 2128